Featured Article

First ^{18}F-Labeled Tracer Suitable for Routine Clinical Imaging of sst Receptor-Expressing Tumors Using Positron Emission Tomography

Margret Schottelius,[1] Thorsten Poethko,[1] Michael Herz,[1] Jean-Claude Reubi,[2] Horst Kessler,[3] Markus Schwaiger,[1] and Hans-Jürgen Wester[1]

[1]Nuklearmedizinische Klinik und Poliklinik, Klinikum rechts der Isar, Technische Universität München, München, Germany; [2]Institute of Pathology, University of Berne, Berne, Switzerland; and [3]Institut für Organische Chemie und Biochemie, Technische Universität München, Garching, Germany

ABSTRACT

Purpose: **Despite excellent radionuclide characteristics, no ^{18}F-labeled peptides are available for quantitative peptide receptor mapping using positron emission tomography (PET) so far, mainly due to time-consuming multistep radiosyntheses with limited overall yields. A newly developed two-step chemoselective conjugation method allows rapid and high-yield [^{18}F]fluorination of peptides via oxime formation and was applied for the synthesis of new ^{18}F-labeled carbohydrated Tyr^3-octreotate (TOCA) analogs with optimized pharmacokinetics suitable for clinical routine somatostatin-receptor (sst) imaging.**

Experimental Design: **^{18}F-labeled glucose (Gluc-*S*-) and cellobiose (Cel-*S*-) derivatives of aminooxy-functionalized TOCA were synthesized via oxime formation with 4-[^{18}F]fluorobenzaldehyde ([^{18}F]FBOA-peptides). Both the *in vitro* internalization profile of Gluc-*S*-Dpr([^{18}F]FBOA)TOCA and Cel-*S*-Dpr([^{18}F]FBOA)TOCA in hsst$_2$-expressing Chinese hamster ovary cells (dual tracer protocol) and their biodistribution in AR42J tumor-bearing mice were investigated and compared with two [^{18}F]fluoropropionylated ([^{18}F]FP) analogs, Gluc-Lys([^{18}F]FP)TOCA and Gluc-*S*-Dpr([^{18}F]FP)TOCA.**

Results: **In contrast to [^{18}F]FP-labeling (3 h), chemoselective [^{18}F]FBOA-formation (50 min) afforded the respective radiopeptides in high yields (65–85%). *In vitro*, Gluc-*S*-Dpr([^{18}F]FBOA)TOCA and Cel-*S*-Dpr([^{18}F]FBOA)-TOCA showed high internalization (139 ± 2 and 163 ± 8 of the reference [^{125}I]Tyr^3-octreotide, respectively), which was reflected by high tumor accumulation *in vivo* [21.8 ± 1.4 and 24.0 ± 2.5% of injected dose/g (1 h), respectively]. However, only Cel-*S*-Dpr([^{18}F]FBOA)TOCA and Gluc-*S*-Dpr([^{18}F]FP)TOCA (tumor: 15.1 ± 1.5% of injected dose/g) with its very low accumulation in all of the nontarget organs showed improved tumor:organ ratios compared with Gluc-Lys([^{18}F]FP)TOCA.ForCel-*S*-Dpr([^{18}F]FBOA)TOCA, tumor:organ ratios (1 h) were 42:1, 27:1, 15:1, 3:1, and 208:1 for blood, liver, intestine, kidney, and muscle, respectively.**

Conclusion: **Due to the fast and high-yield chemoselective radiofluorination strategy and to its excellent pharmacokinetics, Cel-*S*-Dpr([^{18}F]FBOA)TOCA represents the first tracer suitable for routine clinical application in PET somatostatin receptor imaging.**

INTRODUCTION

The success of the ^{111}In-labeled octreotide analog [^{111}In]-octreoscan for *in vivo* detection of somatostatin receptor overexpressing human neoplasms using single photon emission computed tomography (SPECT) is still unchallenged. Compared with single photon emission computed tomography, however, positron emission tomography (PET) represents a superior detection technique with respect to sensitivity, resolution, and quantification. To be able to benefit from these physical advantages, intense research has been directed toward the development of suitable octreotide analogs labeled with positron (β^+) emitting radionuclides during the last decade.

Due to the ease of radiometallation, a variety of chelator-coupled octreotide derivatives have been labeled with positron-emitting radiometals such as ^{86}Y (1–3), ^{64}Cu (4–6), and $^{66/68}$Ga (7–10). Initial patient PET studies using ^{64}Cu-triethylenetetraamine-octreotide as well as [^{66}Ga]DOTA^0-D-Phe^1-Tyr^3-octreotide ([^{66}Ga]DOTATOC) and [^{68}Ga]DOTATOC have been performed recently. Especially the latter two showed excellent imaging characteristics and high tumor:background ratios. [^{86}Y]DOTATOC was successfully applied for dose estimation before peptide receptor-mediated radionuclide therapy (PRRT) using [^{90}Y]DOTATOC (3). Optimization of the chelator moiety with respect to complex stability, radioligand pharmacokinetics, and receptor affinity led to additional very promising TOC analogs for PET as well as PRRT applications (11).

None of the radiometals ^{86}Y, ^{64}Cu, and ^{66}Ga, however, has optimal radionuclide characteristics for routine PET imaging purposes. They suffer from less than optimal half-lives (^{86}Y: 14.7 h, ^{64}Cu: 12.7 h, and ^{66}Ga: 9.49 h), low β^+-percentage branching (^{86}Y: 33%, ^{64}Cu: 18%, and ^{66}Ga: 57%), high β^+-energy (^{86}Y: 1.3 MeV, and ^{66}Ga: 1.7 MeV), as well as coemission of a substantial amount of γ-radiation [^{64}Cu: also β^-

Received 10/13/03; revised 1/30/04; accepted 3/3/04.
Grant support: Deutsche Forschungsgemeinschaft, FOR 411/We 2386/2-1.
The costs of publication of this article were defrayed in part by the payment of page charges. This article must therefore be hereby marked *advertisement* in accordance with 18 U.S.C. Section 1734 solely to indicate this fact.
Requests for reprints: Hans-Jürgen Wester, Nuklearmedizinische Klinik und Poliklinik, Klinikum rechts der Isar, Technische Universität München, Ismaninger Strasse 22, D-81675 München, Germany. Phone: 49-89-4140-4586; Fax: 49-89-4140-4841; E-mail: H.J.Wester@lrz.tum.de.

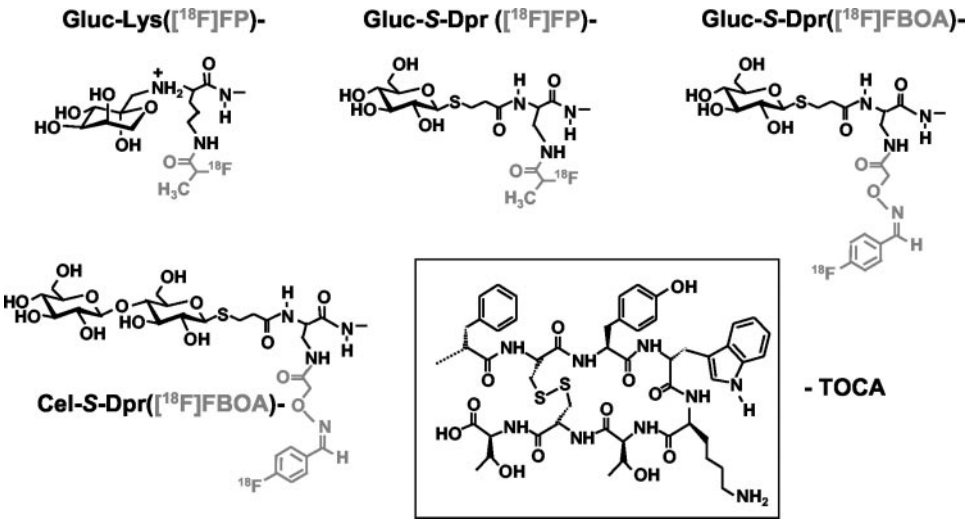

Fig. 1 Structures of Gluc-Lys([^{18}F]FP)-TOCA, Gluc-*S*-Dpr-([^{18}F]FP)TOCA, Gluc-*S*-Dpr-([^{18}F]-FBOA)TOCA, and Cel-*S*-Dpr([^{18}F] FBOA)TOCA.

(37%)], all of which results in increased radiation doses for the patient. Although ^{68}Ga (68 min; 1.8 MeV) already represents a promising radionuclide for PET and, furthermore, is easily accessible by the availability of ^{68}Ge generators, ^{18}F with its half-life of 120 min and low β^+-energy (0.64 MeV) represents the ideal radionuclide for routine PET imaging (12, 13). To exploit these characteristics for PET sst–imaging, ^{18}F-labeled octreotide analogs have been prepared using [^{18}F]fluoroacylation reactions. The first two analogs investigated, 2-[^{18}F]fluoropropionyl-D-Phe^1-octreotide (1, 14) and 4-[^{18}F]fluorobenzoyl-D-Phe^1-octreotide (15) showed low tumor uptake, low tumor retention, and, due to their high lipophilicity, unfavorable biokinetics.

It has been shown recently that sugar conjugation is a powerful method to improve radioligand pharmacokinetics. Carbohydration leads to reduced lipophilicity of small radiolabelled peptides and, thus, to a dramatic reduction of hepatobiliary in favor of renal excretion (16–20). Furthermore, it has been demonstrated that depending on the carbohydrate used tumor uptake of radioiodinated TOC and Tyr^3-octreotate (TOCA) may be substantially increased by glycosylation (19–21).[4] On the basis of these findings, an ^{18}F-labeled sugar analog of TOCA, N^{α}-(1-deoxy-D-fructosyl)-N^{ϵ}-(2-[^{18}F]fluoropropionyl)-Lys^0-Tyr^3-octreotate (Gluc-Lys([^{18}F]FP)-TOCA; Ref. 22) has been developed. To allow both glycosylation and prosthetic group labeling, both of which require a free amino functionality in the peptide, Lys^0 was introduced as a trifunctional linker (Fig. 1). In AR42J tumor-bearing nude mice, Gluc-Lys([^{18}F]FP)-TOCA showed very low hepatic and intestinal uptake, renal excretion, and high tumor accumulation. Initial patient PET studies performed with this radioligand demonstrated excellent tumor:background ratios even at time points $\ll$ 1 h (22).

One significant drawback of Gluc-Lys([^{18}F]FP)-TOCA, especially with respect to clinical routine application, is generally encountered in ^{18}F-labeling of small bioactive peptides via prosthetic groups (1, 13, 14, 23–26): the time consuming, multistep radiosynthesis of the [^{18}F]fluorinated precursor used for prosthetic group labeling, in this case 4-nitrophenyl 2-[^{18}F]fluoropropionate for [^{18}F]fluoroacylation. Furthermore, the presence of a second amino functionality (Lys[5]) in the receptor-binding sequence of TOCA requires the use of a protected precursor peptide, which, in turn, necessitates an additional deprotection and purification step after the [^{18}F]fluoroacylation. This leads to an overall preparation time of Gluc-Lys([^{18}F]FP)-TOCA of ~3 h and, thus, to comparably low radiochemical yields.

To overcome these disadvantages—in this particular case as well as concerning ^{18}F-labeling of peptides and proteins in general—a new strategy ideally allowing both one-step, high-yield synthesis of an ^{18}F-labeled prosthetic group with high stability against *in vivo* defluorination and fast, one-step, chemoselective conjugation with unprotected peptides under mild conditions, preferably in aqueous media, was needed. The chemoselective formation of an oxime bond between a radiohalogenated ketone or aldehyde, *e.g.,* 4-[^{18}F]fluorobenzaldehyde, and a peptide functionalized with an aminooxy-functionality fulfils both requirements. This methodology has already been applied for radioiodination of antibodies (27) and has been proposed for the radioiodination of small peptides (28). Chemoselective oxime ligation has been successfully applied recently in our laboratory for high-yield ^{18}F-labeling of a variety of peptides,[5] including the glycosylated octreotide analogs glucose Gluc-S-Dpr([^{18}F]FBOA)TOCA and cellobiose Cel-S-Dpr([^{18}F]FBOA)TOCA (Fig. 1).

The synthesis and radiolabeling of these radioligands, as well as their evaluation *in vitro* and *in vivo* are presented in

[4] H. J. Wester, M. Schottelius, T. Poethko, K. Bruus-Jensen, and M. Schwaiger. Radiolabelled carbohydrated somatostatin analogs: a brief review of the current status, submitted for publication.

[5] T. Poethko, M. Schottelius, G. Thumshirn, et al. Two-step methodology for high-yield routine radiohalogenation of peptides: ^{18}F-labelled RGD- and octreotide analogs, submitted for publication.

detail in this study. Gluc-Lys([^{18}F]FP)-TOCA was included as a reference. To allow an assessment of the effect of the ^{18}F-labeling method on ligand biodistribution and internalization, an additional [^{18}F]fluoropropionyl-analog, Gluc-*S*-Dpr([^{18}F]FP)TOCA (Fig. 1), was also investigated.

MATERIALS AND METHODS

Peptide Synthesis

General Conditions

Fmoc-(9-fluorenylmethoxycarbonyl-) amino acids as well as *N*-Boc-aminooxyacetic acid were purchased from Novabiochem (Bad Soden, Germany). tritylchloride polystyrene resin was obtained from PepChem (Tübingen, Germany). Solvents and all of the other organic reagents and were purchased from Merck Eurolab (Darmstadt, Germany), Alexis (Grünberg, Germany), Aldrich, or Fluka (Neu-Ulm, Germany).

Solid phase peptide synthesis was carried out manually using a flask shaker (St. John Associates Inc., Beltsville, MD).

Analytical reverse-phase (RP)-high-performance liquid chromatography (HPLC) was performed on a Nucleosil 100 C18 (5 μm; 125 × 4.0 mm) column using a Sykam gradient HPLC System (Sykam GmbH, Fürstenfeldbruck, Germany). The peptides were eluted applying different gradients of 0.1% (v/v) trifluoroacetic acid (TFA) in H_2O (solvent A) and 0.1% TFA (v/v) in acetonitrile (solvent B) at a constant flow of 1 ml/min (specific gradients are cited in the text). UV detection was performed at 220 nm using a 206 PHD UV-Vis detector (Linear Instruments Corporation, Reno, NV). Both retention times, t_R, as well as the capacity factors K′ are cited in the text. K′ is calculated as follows:

$$K' = \frac{t_R - t_0}{t_0}$$

where

$$t_R = \text{retention time}$$

and

$$t_0 = \frac{\text{dead volume of the column (ml)}}{\text{flow (ml} \times \text{min}^{-1})}$$

Preparative RP-HPLC was performed on the same HPLC system using a Multospher 100 RP 18–5 (250 × 10 mm) column at a constant flow of 5 ml/min.

Mass spectra were recorded on the liquid chromatography-mass spectroscopy system LCQ from Finnigan (Bremen, Germany) using the Hewlett Packard series 1100 HPLC system.

Synthesis of Small Organic Precursors

***S*-(2,3,4,6-Tetraacetyl-glucosyl)-Mercaptopropionic Acid Pentafluorophenyl Ester.** *S*-(2,3,4,6-tetraacetyl-glucosyl)-mercaptopropionic acid was synthesized from peracetylated glucose and 3-mercaptopropionic acid using $BF_3{\cdot}Et_2O$ as an activator (29). The pentafluorophenyl activated ester was obtained by reaction of the free acid with pentafluorophenol (1.1 eq) in the presence of *N*,*N*′-diisopropyl carbodiimide (1.1 eq). The overall yield was 62%.

^{1}H NMR ($CDCl_3$): d (ppm) 2.04 (3 H, s), 2.06 (3 H, s), 2.09 (3 H, s), 2.11 (3 H, s), 2.98–3.14 (4 H, m, SCH_2CH_2), 3.74–3.81 (1 H, m), 4.16–4.30 (2 H, m), 4.60 (1 H, d, J = 10 Hz), 5.05–5.16 (2 H, m), 5.25 (1 H, d, J = 9.5 Hz).

S-1-Heptaacetyl-Cellobiosyl-Mercaptopropionic Acid Pentafluorophenyl Ester. Synthesis was performed in analogy to the glucose-derivative. The overall yield was 48%.

Calculated monoisotopic mass for S-1-heptaacetyl-cellobiosyl-mercaptopropionic acid pentafluorophenyl ester ($C_{35}H_{39}O_{19}SF_5$): 890.2; found: m/z = 913.2 $[M+Na]^+$, 1802.4 $[2M+Na]^+$.

^{1}H-NMR ($CDCl_3$): d (ppm) 1.96 (3 H, s), 1.99 (3 H, s), 2.00 (3 H, s), 2.01 (3 H, s), 2.03 (3 H, s), 2.06 (3 H, s), 2.09 (3 H, s), 2.89–3.05 (4 H, m, SCH_2CH_2), 3.58–3.67 (2 H, m), 3.71–3.76 (2 H, m), 4.00–4.11 (2 H, m), 4.32–4.39 (1 H, m), 4.48–4.55 (2 H, m), 4.87–5.22 (5 H, m).

Peptide Synthesis

Glycosylated Precursors for Chemoselective Reaction with 4-[^{18}F]Fluorobenzaldehyde

Fmoc-Dpr^0-Tyr^3-Lys^5(Dde)-Octreotate. The synthesis of Fmoc-Dpr^0-Tyr^3-Lys^5 (Dde)-octreotate was performed as described previously for TOCA(Dde) (20). Briefly, the peptide sequence Fmoc-Dpr(Boc)-DPhe-Cys(Trt)-Tyr(tBu)-DTrp(Boc)-Lys(Dde)-Thr(tBu)-Cys(Trt)-Thr(tBu)-OH was assembled on tritylchloride polystyrene resin according to standard Fmoc protocol. Amino acid coupling was performed using 1-hydroxybenzotriazole (1.5 eq) and *O*-(1H-benzotriazol-1-yl)-N,N,N′,*N*′-tetramethyluronium-tetrafluoroborate (1.5 eq) as coupling reagents and (*N*-ethyldiisopropylamine (4 eq) as a base. The peptide was cleaved from the solid support using 95% TFA, 2.5% triisobutylsilane, and 2.5% H_2O. Disulfide bridge formation was achieved using H_2O_2 in a tetrahydrofurane/5 mM NH_4OAc mixture buffered to pH 7 with saturated $NaHCO_3$. Yield based on resin-bound Thr: 74%

HPLC (40→100% B in 15 min): t_R = 7.8 min; K′ = 3.32.

Calculated monoisotopic mass for Fmoc-Dpr^0-Tyr^3-Lys^5 (Dde)-octreotate ($C_{77}H_{92}N_{12}O_{17}S_2$): 1520.6

found: m/z = 1521.7 $[M+H]^+$, 1543.8 $[M+Na]^+$, 1559.6 $[M+K]^+$

Coupling with* N-*(Boc)-Aminooxyacetic Acid, Glycosylation, and Deprotection. *N*-(Boc)-aminooxyacetic acid was coupled to Fmoc-Dpr^0-Tyr^3-Lys^5 (Dde)-octreotate under optimized coupling conditions (1-hydroxy-7-azabenzotriazole, *N*,*N*′-diisopropyl carbodiimide, and pyridine; Ref. 30). After subsequent Fmoc-deprotection using 20% piperidine in DMF, N_2-terminal glycosylation was achieved by reaction with Gluc(4Ac)/S-1-heptaacetyl-cellobiosyl-mercaptopropionic acid pentafluorophenyl ester (1.1 eq) in the presence of *N*-ethyldiisopropylamine (1.1 eq). Dde deprotection of the Lys^5 side chain was performed using 2% hydrazine hydrate in DMF, followed by removal of the acetyl protecting groups in the sugar moiety using potassium cyanide in methanol (31). After final Boc-deprotection of the aminooxy-functionality using 50% TFA in dichloromethane (10 min), the peptides were purified using preparative RP-HPLC.

Gluc-*S*-Dpr(Aoa)-TOCA: HPLC (15→45% B in 15 min): t_R = 10.1 min; K′ = 5.17.

Calculated monoisotopic mass for Gluc-*S*-Dpr(Aoa)-TOCA ($C_{63}H_{87}N_{13}O_{21}S_3$): 1457.5

found: m/z = 1458.6 $[M+H]^+$, 1480.5 $[M+Na]^+$, 1496.4 $[M+K]^+$

Cel-*S*-Dpr(Aoa)-TOCA: HPLC (15→45% B in 15 min): t_R = 9.6 min; K′ = 4.98.

Calculated monoisotopic mass for Cel-*S*-Dpr(Aoa)-TOCA ($C_{69}H_{97}N_{13}O_{26}S_3$): 1619.6

found: m/z = 1620.5 $[M+H]^+$, 1642.4 $[M+Na]^+$, 1658.4 $[M+K]^+$

Glycosylated Precursors for Reaction with 4-Nitrophenyl-2-[^{18}F]Fluoropropionate

N$_\alpha$-(1-deoxy-D-fructosyl)-Lys^0-Tyr^3-Lys^5(Dde)-octreotate [Gluc-Lys-TOCA(Dde)]. Tyr^3-Lys^5(Dde)-octreotate [TOCA(Dde)] was synthesized via SPPS as cited above. After cyclization, Fmoc-Lys(Boc)-OH was coupled to the N-terminus in solution using standard coupling conditions, followed by Fmoc-deprotection (20% piperidine in DMF) and subsequent Amadori reaction with glucose in a methanol/AcOH solvent system (32). Final Boc-deprotection was carried out using a mixture of 95% TFA, 2.5% triisobutylsilane, and 2.5% H_2O.

Gluc-Lys-TOCA(Dde): HPLC (30→80% B in 15 min): t_R = 4.7 min; K′ = 3.25.

Calculated monoisotopic mass for Gluc-Lys-TOCA(Dde) ($C_{71}H_{98}N_{12}O_{20}S_2$): 1502.6

found: m/z = 1503.7 $[M+H]^+$, 1525.7 $[M+Na]^+$.

Gluc-S-Dpr^0-Tyr^3-Lys^5(Dde)-Octreotate [Gluc-S-Dpr-TOCA(Dde)]. Solution phase coupling of Fmoc-Dpr(Boc)-OH to TOCA(Dde) was followed by NH_2-terminal Fmoc-deprotection (20% piperidine in DMF). Subsequent conjugation with *S*-(2,3,4,6-tetraacetyl-glucosyl)-mercaptopropionic acid pentafluorophenyl ester, sugar deacetylation, and Boc-deprotection were carried out as outlined for the Aoa-containing analogs.

Gluc-*S*-Dpr-TOCA(Dde): HPLC (30→60% B in 15 min): t_R = 6.8 min; K′ = 3.42.

Calculated monoisotopic mass for Gluc-*S*-Dpr-TOCA(Dde) ($C_{71}H_{96}N_{12}O_{21}S_3$): 1548.6

found: m/z = 1549.7 $[M+H]^+$, 1571.5 $[M+Na]^+$.

Synthesis of the Reference Compounds

FBOA-Derivatives. Gluc/Cel-*S*-Dpr(Aoa)-TOCA was dissolved in a 1:1 (v/v) mixture of H_2O/methanol, and an equimolar amount of 4-fluorobenzaldehyde was added. After 30 min at 60°C, the coupling product was purified using RP-HPLC.

Gluc-*S*-Dpr(FBOA)TOCA: HPLC (20→70% B in 15 min): t_R = 10.2 min; K′ = 5.81.

Calculated monoisotopic mass ($C_{70}H_{90}N_{13}O_{21}S_3F$): 1563.5. found: m/z = 1564.5 $[M+H]^+$, 1602.3 $[M+K]^+$.

Cel-*S*-Dpr(FBOA)TOCA: HPLC (20→70% B in 15 min): t_R = 10.0 min; K′ = 5.12.

Calculated monoisotopic mass ($C_{76}H_{100}N_{13}O_{26}S_3F$): 1725.6. found: m/z = 1726.6 $[M+H]^+$, 1748.4 $[M+Na]^+$, 1764.3 $[M+K]^+$.

2-Fluoropropionyl Derivatives. Coupling of 2-fluoropropionic acid (33) to the unprotected amino functionality of Gluc-Lys-TOCA(Dde) and Gluc-*S*-Dpr-TOCA(Dde) was carried out using standard conditions (1-hydroxybenzotriazole, *O*-(1H-benzotriazol-1-yl)-*N*,*N*,*N*′,*N*′-tetramethyluronium-tetrafluoroborate, and *N*-ethyldiisopropylamine). After removal of the Lys^5-Dde-protecting group using 2% hydrazine hydrate in DMF, the peptides were isolated using preparative RP-HPLC.

Gluc-Lys(N_ϵ-2-fluoropropionyl)-TOCA.

HPLC (20→50% B in 15 min): t_R = 12.9 min; K′ = 8.3.

Calculated monoisotopic mass ($C_{64}H_{89}N_{12}O_{19}S_2F$): 1412.6. found: m/z = 1413.4 $[M+H]^+$, 1435.5 $[M+Na]^+$, 1451.3 $[M+K]^+$.

Gluc-*S*-Dpr(N_β-2-fluoropropionyl)-TOCA (Gluc-*S*-Dpr-(FP)TOCA).

HPLC (20→50% B in 15 min): t_R = 9.6 min; K′ = 4.80.

Calculated monoisotopic mass ($C_{64}H_{87}N_{12}O_{20}S_3F$): 1458.5. found: m/z = 1459.5 $[M+H]^+$, 1481.4 $[M+Na]^+$, 1497.3 $[M+K]^+$.

Radiolabeling

Instrumentation

Radio-HPLC was performed using a Sykam gradient system (Sykam GmbH, Fürstenfeldbruck, Germany) and an UVIS 200 photometer (Linear Instruments Corporation, Reno, NV). For radioactivity measurement, the outlet of the UV-photometer was connected to a Na(Tl) well-type scintillation counter Ace Mate 925-Scint (EG & G Ortec, München, Germany).

^{18}F-Labeling Using 4-[^{18}F]Fluorobenzaldehyde

The synthesis of 4-[^{18}F]fluorobenzaldehyde from 4-formyl-*N*,*N*,*N*-trimethylanilinium triflate was performed as described previously (34). For peptide labeling, a solution of Gluc/Cel-*S*-Dpr(Aoa)-TOCA (0.11 μmol) in 100 μl water was added to 500 μl of a freshly prepared methanolic 4-[^{18}F]fluorobenzaldehyde solution. Trifluoroacetic acid (2%; 8 μl) was added to adjust the pH to 2. After 10 min at 60°C and preparative HPLC [column: YMC RP 18 s-4 μm 80A, 150 × 20 mm (YMC Europe), gradient: 0% B for 5 min, then 15–50% B in 20 min, 10 ml flow] overall radiochemical yields (not optimized) of Gluc/Cel-*S*-Dpr([^{18}F]FBOA)-TOCA were about 40–60% in an overall synthesis time of ~50 min.

^{18}F-Labeling Using 4-Nitrophenyl 2-[^{18}F]Fluoropropionate

The synthesis of 4-nitrophenyl 2-[^{18}F]fluoropropionate was carried out according to the literature (14). For ^{18}F-acylation, the respective Lys^5(Dde)-protected peptide (1.3–1.5 mg) was dissolved in 180–200 μl of DMSO, and 2 μl of *N*-ethyldiisopropylamine were added. The resulting solution was added to a vial containing no carrier added (n.c.a.) 4-nitrophenyl 2-[^{18}F]fluoropropionate. The mixture was heated to 70°C for 15 min. After analytical HPLC reaction control, 4 μl of hydrazine hydrate were added to the solution containing the [^{18}F]fluoroacylated peptide. The deprotected peptide was then isolated via preparative HPLC (Multospher 100 RP18–5, 250 × 10 mm; linear gradient 22–30% B in 30 min, flow rate 5 ml/min, t_R = 15–17 min; K′ = 7).

Radiochemical yields (based on 4-nitrophenyl 2-[^{18}F]fluoropropionate) of N$^\alpha$-(1-deoxy-D-fructosyl)-N$^\epsilon$-(2-[^{18}F]fluoropropionyl)-Lys^0-Tyr^3-octreotate [Gluc-Lys([^{18}F]FP)-TOCA] and Gluc-*S*-Dpr(N_β-2-[^{18}F]fluoropropionyl)-TOCA Gluc-*S*-Dpr([^{18}F]FP)TOCA were ~25% in a synthesis time of 1 h.

Radioiodination

Radioiodination of Gluc-*S*-Dpr(FP)TOCA, Gluc-*S*-Dpr-(FBOA) BOA)TOCA, Cel-*S*-Dpr(FBOA)-TOCA, and the reference TOC was performed using the Iodogen method.

A solution of 100–200 μg of peptide in 200 μl of PBS (0.1 M; pH 7.4) was transferred to an Eppendorf cap coated with 30 μg of Iodogen (Pierce, Rockford, IL). After the addition of 5–20 μl of solution of radioiodide (Amersham, Buckinghamshire, United Kingdom) in 0.05 M NaOH {[^{125}I]NaI (n.c.a.): 18–74 MBq, [^{123}I]NaI (c.a.): 37–185 MBq} the cap was vortexed, and the labeling reaction was allowed to proceed for 15–20 min at room temperature. The peptide solution was then removed from the insoluble oxidizing agent.

The radioiodinated peptides were purified via RP-HPLC [column: Nucleosil 100 C18, 5 μm, 125 × 4.0 mm (CS GmbH, Langerwehe, Germany), flow rate: 1 ml/min]. Isocratic solvent mixtures containing 28% ([^{125}I]TOC), 32% ([^{123}I]Gluc-*S*-Dpr(FP)TOCA), 41% {[^{123}I]Cel-*S*-Dpr(FBOA)TOCA}, or 42% {[^{123}I]Gluc-*S*-Dpr(FBOA)TOCA} ethanol (0.5% AcOH) in water (0.5% AcOH) were used. Radiochemical yields after purification ranged from 45% to 65%. Radiochemical purities were >98% for all of the radioiodinated peptides.

For the paired label internalization experiments, the collected HPLC fractions of both [^{125}I]TOC and the respective ^{123}I-labeled radioligand were each evaporated to dryness. The radiopeptides were redissolved in assay medium (containing 5% BSA) and diluted to an activity concentration of ~200,000 cpm/10 μl. A 1:1 (v/v) mixture of both solutions containing ~100,000 cpm/10 μl of each radioligand was then used for the internalization experiment.

Lipophilicity

To a solution of ~2 kBq of radiolabelled peptide in 500 μl of PBS (pH 7.4), 500 μl of octanol were added ($n = 6$). Vials were vortexed vigorously for 3 min. To achieve quantitative phase separation, the vials were centrifuged at 14,600 × *g* for 6 min in a Biofuge 15 (Heraeus Sepatech, Osterode, Germany). The activity concentrations in 100 μL samples of both the aqueous and the organic phase were measured in a gamma counter. Both the partition coefficient P_{ow}, which is defined as the molar concentration ratio of a single species A between octanol and water at equilibrium, and log P_{ow}, which is an important parameter used to characterize lipophilicity of a compound (35), were calculated.

In Vitro Studies

Cell Culture

Chinese hamster ovary (CHO) cells stably transfected with human sst_2 (epitope tagged at the N-terminal end) were kindly provided by Dr. Jenny Koenig, University of Cambridge, Cambridge, United Kingdom. Cells were grown in DMEM/Nutrition Mix F-12 with Glutamax-I (1:1); (Gibco BRL) supplemented with 10% FCS and 500 mg/l Geneticin (Gibco BRL). AR42J cells were obtained from European Collection of Animal Cell Cultures (Salisbury, United Kingdom). Cells were maintained in RPMI 1640 (Seromed, Berlin, Germany) supplemented with 10% FCS (Seromed) and 2 mM L-glutamine (Gibco BRL, Life Technologies, Inc., Karlsruhe, Germany). Cultures were maintained at 37°C in a 5% CO_2/humidified air atmosphere.

In the assay medium used for the internalization studies, FCS was replaced by 1% BSA (Sigma, St. Louis, MO).

For cell counting, a CASY 1-TT cell counter and analyzer system (Schärfe System GmbH, Reutlingen, Germany) was used.

Internalization and Determination of $EC_{50,R}$

Experiments were performed as described in detail previously.[6] Briefly, after preconditioning of the cells (~100.000 cells/well) with 190 μl of unsupplemented medium for a minimum of 15 min, 50 μl (per well) of DMEM (5% BSA) containing increasing concentrations of unlabeled TOC were added, followed by the addition of ~100,000 cpm of both the respective ^{123}I-labeled glycosylated peptide and of the reference [^{125}I]TOC in 10 μl of DMEM (5% BSA). Final TOC-concentrations in the incubation medium used for the determination of the $EC_{50,R}$ were 0.1, 0.2, 0.5, 0.8, 1, 2, 4, 6, 8, 10, 12, 15, 20, 50, 100, 500, and 1000 nM. In a control experiment (n.c.a. conditions), TOC-free DMEM (5% BSA) was added. Nonspecific internalization was determined by including 5 μM unlabelled TOC. Experiments were carried out in triplicate for each concentration. Because internalization of [^{125}I]TOC and its analogs into the CHO cells used is very fast (up to 15–35% of the applied activity within 10 min), the incubation time used for all of the internalization experiments described here has also been limited to 10 min.

After incubation at 37°C, the incubation medium was removed, and cells were rinsed with 250 μl of fresh medium. The combined medium fractions represent the amount of free radioligand. Receptor-bound (acid releasable) radioactivity was then removed using 2 × 250 μl of ice cold acid wash buffer (0.02 M NaOAc buffered with AcOH to pH = 5). The internalized activity was released by incubation with 250 μl of 1 N NaOH, transferred to vials, and combined with 250 μl of PBS used for rinsing the wells. Quantification of the amount of free, acid-releasable, and internalized activity was performed in a gamma counter.

For numerical analysis of the EC_{50} of TOC for internalization, data for both the ^{123}I-labeled compound of interest and for the reference [^{125}I]TOC in the same experiment were first corrected by the amount of nonspecific internalization, respectively, and then each normalized to the amount of internalized ligand in the absence of unlabelled competitor (100%). Data were fitted with a weighted two-parameter logistic function using SigmaPlot. To eliminate the influence of cell count and cell viability on the absolute EC_{50}-values, data are expressed as the ratio ($EC_{50,R}$) of the EC_{50} observed for the compound of interest and the EC_{50} found for [^{125}I]TOC in the same experiment [$EC_{50,R}$ = EC_{50} (compound of interest)/EC_{50} ([^{125}I]TOC)].

[6] M. Schottelius, J. C. Reubi, M. Schwaiger, and H. J. Wester. N-terminal sugar conjugation and C-terminal Thr(ol)-for-Thr exchange in radioiodinated Tyr^3-octreotide: effect on cellular ligand trafficking in vitro and tumor accumulation in vivo, submitted for publication.

Externalization and Recycling

As in the previous experiment, cells were incubated with the respective ^{123}I-labeled peptide and the reference [^{125}I]TOC at 37°C for 10 min and washed with medium. To ensure receptor integrity, no acid wash was performed after this initial internalization incubation. Then, to determine the extent of ligand recycling, two different experiments were performed. In the experiment allowing ligand recycling, 200 μl of assay medium and 50 μl of medium (5% BSA) were added to each well. In the experiment inhibiting ligand recycling, 200 μl of assay medium and 50 μl of medium (5% BSA) containing 25 μM TOC were added to each well. Experiments were carried out in triplicate for both experimental conditions. Subsequently, the cells were incubated at 37°C for 30 and 60 min, respectively. The supernatant was removed and combined with 250 μl of medium used for rinsing the cells. This fraction represents the amount of externalized ligand. The following acid wash and lysis of the cells was performed as described for the internalization experiment.

Affinity Profiles to hsst

Cell membrane pellets of cells stably expressing human sst_1, sst_2, sst_3, sst_4, and sst_5 (sst_1 and sst_5: CHO-K1 cells; sst_{2-4}: CCL39 cells) were prepared, and receptor autoradiography was performed on pellet sections (mounted on microscope slides), as described in detail previously (36). Displacement experiments were performed with the universal somatostatin radioligand ^{125}I-[Leu^8, D-Trp^{22}, Tyr^{25}]-somatostatin 28 using increasing concentrations of Gluc-Lys([^{19}F]FP)TOCA, Gluc-*S*-Dpr([^{19}F]FP)TOCA, Gluc-*S*-Dpr([^{19}F]FBOA)TOCA, Cel-*S*-Dpr([^{19}F]FBOA)TOCA, 3-iodo-Tyr^3-octreotide, and the reference somatostatin 28 (0.1–1000 nM). IC_{50} values were calculated after quantification of the data using a computer-assisted image processing system.

In Vivo Studies

Tumor Model

The AR42J cell line as a transplantable rat pancreatic tumor model with high sst_2 expression (37) was used. To establish tumor growth, cells were detached from the surface of the culture flasks using 1 mM EDTA in PBS, centrifuged, and resuspended in serum-free culture medium. Concentration of the cell suspension was 2.5–5 $\times$ 10^6 cells/100 μl serum. Nude mice (female, 6–8 weeks) were injected with 100 μl of the cell suspension s.c. into the flank. Ten days after tumor transplantation all of the mice showed solid palpable tumor masses (tumor weight 200–900 mg) and were used for the experiments.

Biodistribution Studies

The radiolabeled peptides [40–60 μCi in 100 μl PBS (pH 7.4)], were injected i.v. into the tail vein of AR42J tumor-bearing nude mice. For competition studies, 0.4 or 0.6 mg/kg TOC (10 or 15 μg/mouse) were coinjected. The animals (groups of 3–5) were sacrificed 10 and 60 min after injection, and the organs of interest were dissected. The radioactivity was measured in weighted tissue samples using a gamma counter.

PET Imaging

For PET imaging, the ^{18}F-labeled peptides [35–77 μCi in 100–200 μl PBS (pH 7.4)], were injected i.v. into the tail vein of AR42J tumor-bearing nude mice. For competition studies, 0.6 mg/kg TOC (15 μg/mouse) were coinjected. After 60 min, mice were either euthanized {Gluc-*S*-Dpr([^{18}F]FP)TOCA} or anaesthetized using a xylazine/ketamine combination. Static PET images (20 min; 5 min transmission; zoom 3.0) were acquired using an Siemens EXACT HR Plus scanner. The axial resolution of the scanner at full-width at half-maximum is ~5 mm, the transaxial resolution is ~8 mm. Images were reconstructed by iterative reconstruction (8 iterations, 4 subsets). For the quantification of tumor:kidney ratios, ROI [region of interest] analysis was performed in a minimum of 2 coronal slices/mouse.

RESULTS

Synthesis. Standard Fmoc solid phase peptide synthesis afforded TOCA(Dde) in yields >85% (based on resin-bound Thr^1). After quantitative N-terminal solution phase coupling with Fmoc-Lys(Boc) or Fmoc-Dpr(Boc) and subsequent Fmoc-deprotection, the peptides were either glycosylated via Amadori reaction [Gluc-Lys-TOCA(Dde)] or via conjugation with the pentafluorophenyl active esters of *S*-(tetraacetyl-glucosyl)- or *S*-(heptaacetyl-cellobiosyl)-3-mercaptopropionic acid. As determined via RP-HPLC reaction control, yields of Amadori-glycosylation never exceeded 80% within 16 h at 60°, whereas the latter reaction was quantitative within 30–45 min at room temperature.

Initially, Dpr-sidechain acylation with Boc-protected 2-aminooxyacetic acid [*N*-(Boc)-aminooxyacetic acid] was performed using a large excess (10 eq) of *N*-(Boc)-aminooxyacetic acid and coupling reagents [1-hydroxybenzotriazole/*O*-(1H-benzotriazol-1-yl)-*N*,*N*,*N*′,*N*′-tetramethyluronium-tetrafluoroborate] over Dpr-deprotected peptide. Even under these conditions, coupling yields were comparably low (<80% as determined via HPLC reaction control). In contrast, using 1-hydroxy-7-azabenzotriazole/*N*,*N*′-diisopropyl carbodiimide (1.5 eq) as coupling reagents and pyridine as a base (30) led to quantitative *N*-(Boc)-aminooxyacetic acid-functionalization.

Whereas both precursors for [^{18}F]fluoropropionylation, Gluc-Lys-TOCA(Dde) and Gluc-*S*-Dpr-TOCA(Dde), were obtained in yields of ~20% (based on nonglycosylated peptide) after deprotection and purification via preparative HPLC, yields of Aoa-functionalized peptides were low (2–5%). Due to the high reactivity of the Aoa-group (38), side product formation during preparative HPLC necessitated additional purification steps and reduced final product purity (UV trace in HPLC at 220 nm) to 80–85%.

Radiolabeling. Both n.c.a. 4-nitrophenyl-2-[^{18}F]fluoropropionate (14) and n.c.a. 4-[^{18}F]fluorobenzaldehyde (34; see footnote 5) were synthesized as described.

After [^{18}F]fluoroacylation, *in situ* Dde-deprotection, and subsequent RP-HPLC purification, radiochemical yields of Gluc-Lys([^{18}F]FP)TOCA and Gluc-*S*-Dpr([^{18}F]FP)TOCA based on 4-nitrophenyl-2-[^{18}F]fluoropropionate ranged from 25% to 45% (d.c.), whereas one-step conjugation with 4-[^{18}F]fluorobenzaldehyde, followed by RP-HPLC isolation, afforded Gluc-*S*-Dpr([^{18}F]FBOA)TOCA and Cel-*S*-Dpr([^{18}F]-

Table 1 Lipophilicities (log P_{ow}) of the four ^{18}F-labeled TOCA[a] analogs investigated in this study

Values are mean ± SD (n = 6).

	log P_{OW}
Gluc-Lys([^{18}F]FP)TOCA	−1.70 ± 0.03
Gluc-*S*-Dpr([^{18}F]FP)TOCA	−2.80 ± 0.01
Gluc-*S*-Dpr([^{18}F]FBOA)TOCA	−1.24 ± 0.03
Cel-*S*-Dpr([^{18}F]FBOA)TOCA	−1.70 ± 0.03

[a]TOCA, Tyr^3-octreotate.

FBOA)TOCA in 60–80% radiochemical yield. Overall preparation times for the [^{18}F]FP- and the [^{18}F]FBOA-labeled peptides were 3 h and 50 min, respectively. Radiochemical purities of all of the ^{18}F-labeled peptides (n.c.a.) were >98%.

Usually, the amount of ^{18}F-labeled peptide produced was below the UV-detection limit during HPLC, which impeded estimation of the specific activity of the respective radioligand. Because this is indispensable for an approximate estimation of the concentration of radioligand used in the internalization assays, however, not the ^{18}F-labeled compounds, but the corresponding ^{123}I-labeled ^{19}F-reference compounds Gluc-*S*-Dpr(FP)TOCA, Gluc-*S*-Dpr(FBOA)TOCA, and Cel-*S*-Dpr(FBOA)TOCA were used in the *in vitro* experiments. This strategy not only affords radioligands with comparable specific activity but, furthermore, ensures comparability of the data obtained for the new fluoro-analogs with those obtained for other radioiodinated glyco-analogs of octreotide in a previous study.[6] On the basis of the fairly similar sst_2-affinities of TOC and radioiodinated TOC (Table 2), an effect of radioiodination on the internalization characteristics of the ^{123}I-labeled fluoro-analogs investigated was assumed to be negligible.

Radioiodination of Gluc-*S*-Dpr(FP)TOCA, Gluc-*S*-Dpr-(FBOA)TOCA, and Cel-*S*-Dpr(FBOA)TOCA, as well as the reference TOC for the *in vitro* internalization assays afforded the respective $^{123/125}$I-labeled peptides in radiochemical yields of 45–75% after RP-HPLC purification. All of the radioiodinated peptides were obtained in high radiochemical purity (>99%). Because the HPLC conditions applied allowed efficient separation of the radioiodinated product from the unlabelled precursor ($\Delta t_R \geq 4$ min) for all of the radioiodinated analogs investigated, and because no coeluting carrier peak was observed in the quality control UV-chromatogram, the specific activity of the labeled peptides was assumed to be that of the radioiodide used for their preparation (≥2000 Ci/mmol for ^{125}I, ≈5000 Ci/mmol for ^{123}I).

Lipophilicity. Lipophilicities of the four compounds investigated are listed in Table 1. Despite the loss of the positive charge on N_α of D-Phe^1 (Fig. 1), the lipophilicity of Gluc-*S*-Dpr([^{18}F]FP)TOCA is substantially lower than that of Gluc-Lys([^{18}F]FP)TOCA. Substitution of the small [^{18}F]FP moiety by the aromatic [^{18}F]FBOA residue, however, leads to a strongly increased lipophilicity of Gluc-*S*-Dpr([^{18}F]FBOA)TOCA compared with Gluc-*S*-Dpr([^{18}F]FP)TOCA (log P_{ow} = −1.24 ± 0.03 *versus* −2.80 ± 0.01, respectively). This effect is partly compensated for by replacement of the monosaccharide glucose by the more hydrophilic disaccharide cellobiose in Cel-*S*-Dpr([^{18}F]-FBOA)TOCA, leading to an intermediate log P_{ow} identical to the value found for Gluc-Lys([^{18}F]FP)TOCA.

***In Vitro* Studies.** For all four of the^{18}F-labeled peptides investigated the *in vitro* binding profile to human sst_{1-5} has been determined (Table 2). The corresponding ^{19}F reference compounds all showed very high $hsst_2$ affinity comparable with that of native somatostatin 28, including no affinity to $hsst_1$, very low affinity to $hsst_3$, and moderate affinity to $hsst_4$ and $hsst_5$. Compared with iodinated Tyr^3-octreotide, which is used as the internal reference in the dual tracer internalization studies performed in this study, the $hsst_2$ affinity of Gluc-Lys(FP)-TOCA, Gluc-*S*-Dpr(FP)TOCA, and Gluc-*S*-Dpr(FBOA)TOCA is decreased by a factor of two, whereas it is comparable for the Cel-*S*-Dpr(FBOA) analog. Of the four compounds, Gluc-Lys(FP)-TOCA showed the highest and Cel-*S*-Dpr(FBOA)-TOCA the lowest sst_2-receptor specificity.

For [^{123}I]Gluc-*S*-Dpr(FP)TOCA, [^{123}I]Gluc-*S*-Dpr(FBOA)-TOCA, and [^{123}I]Cel-*S*-Dpr(FBOA)TOCA the amount of activity internalized into $hsst_2$-expressing CHO cells was determined in dual tracer experiments (internal reference = [^{125}I]TOC) both in the absence (control) or the presence of increasing concentrations of unlabelled TOC (0.1 − 1000 nM; Fig. 2). Data were corrected by the nonspecific internalization (determined by coincubation with 5 μM TOC) and normalized to maximum internalization (control = 100%). The higher the amount of cold TOC needed to reduce cellular uptake of the respective ^{123}I-labeled compound as well as the internal reference [^{125}I]TOC to 50% of maximum internalization (EC_{50} for internalization), the higher, in a first approximation, the receptor affinity of the ligand. To eliminate interexperimental inaccuracies in cell count or cell viability, data are generally cited

Table 2 Affinity profiles (IC_{50}) to the human sst1-sst5 receptors determined for somatostatin 28[a] and the compounds investigated using ^{125}I-[Leu^8, D-Trp^{22}, and Tyr^{25}]-somatostatin 28 as the radioligand

Values are IC_{50} ± SD [nM], number of experiments in parentheses. Cell membrane pellets were prepared from CHO-K1 cells (sst_1 and sst_5) and CCL39 cells (sst_{2-4}; Ref. 36).

Peptide	sst1	sst2	sst3	sst4	sst5
SS-28	3.6 ± 0.3 (5)	2.1 ± 0.3 (5)	3.2 ± 0.2 (5)	3.0 ± 0.3 (5)	2.5 ± 0.2 (5)
TOC	>1,000 (2)	3.1 ± 1.8 (2)	330 ± 146 (2)	346 ± 114 (2)	10.8 ± 1.8 (2)
I-TOC	>10,000 (3)	1.3 ± 0.3 (3)	128 ± 22 (3)	867 ± 33 (3)	50 ± 12 (3)
Gluc-Lys([^{19}F]FP)TOCA	>10,000 (3)	2.8 ± 0.4 (3)	>1,000 (3)	437 ± 84 (3)	123 ± 8.8 (3)
Gluc-*S*-Dpr([^{19}F]FP)TOCA	>1,000 (2)	2.7 ± 2.1 (2)	742 ± 182 (2)	339 ± 11 (2)	87 ± 18 (2)
Gluc-*S*-Dpr([^{19}F]FBOA)TOCA	>1,000 (2)	2.5 ± 1.3 (2)	692 ± 108 (2)	298 ± 52 (2)	74 ± 20 (2)
Cel-*S*-Dpr([^{19}F]FBOA)TOCA	>1,000 (2)	1.8 ± 1.1 (2)	707 ± 30 (2)	339 ± 163 (2)	45 ± 1 (2)

[a]SS 28, somatostatin 28.

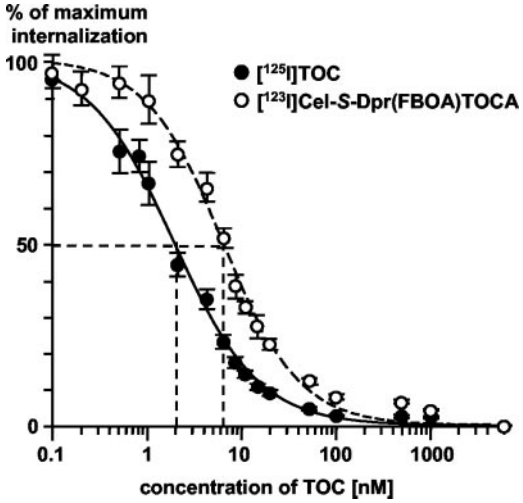

Fig. 2 Exemplary determination of $EC_{50,R}$ [= EC_{50} ([^{123}I]Cel-*S*-Dpr(FBOA)TOCA)/EC_{50} ([^{125}I]TOC)] of [^{123}I]Cel-*S*-Dpr(FBOA)-TOCA in Chinese hamster ovary cells stably expressing $hsst_2$. Internalization of each compound is first corrected by nonspecific internalization (5 μM TOC) and then normalized to maximum internalization (control = no TOC added; $n = 3$); *bars,* ±SD.

as the normalized $EC_{50,R} = EC_{50}$(^{123}I-labeled analog)/EC_{50}([^{125}I]-TOC; $n = 3$).

As summarized in Table 3, both [^{123}I]Gluc-*S*-Dpr(FBOA)-TOCA and [^{123}I]Cel-*S*-Dpr(FBOA)TOCA show substantially enhanced internalization compared with [^{125}I]TOC (140–160%). For both analogs, increased internalization is paralleled by very high $EC_{50,R}$ values (3.2–4.1). In contrast, [^{123}I]Gluc-*S*-Dpr(FP)TOCA shows the highest internalization of the compounds investigated (190.2 ± 6.6% of the reference) but a comparably low $EC_{50,R}$.

To assess the extent of ligand externalization and subsequent reinternalization, *i.e.,* ligand recycling, cells were first incubated with the respective radioligands for 10 min to allow intracellular ligand accumulation. After replacement of the incubation medium with ligand-free medium, the amount of activity released into the medium over time was quantified both in the absence (conditions allowing recycling) and in the presence of 5 μM TOC (conditions inhibiting recycling). Fig. 3 illustrates the exemplary externalization kinetics of [^{123}I]Cel-*S*-Dpr(FBOA)-TOCA and [^{125}I]TOC under both experimental conditions. When reinternalization was allowed, the amount of [^{125}I]TOC and of all of the ^{123}I-labeled derivatives released into the medium within 60 min was nearly identical (21–29% of the activity that was cellularly located after the internalization incubation; data not shown). When recycling was inhibited, 96–97% of the cellular activity were externalized into the medium in the case of all of the ^{123}I-labeled sugar analogs ([^{125}I]TOC: 92–93%) over the 60-min observation period.

***In Vivo* Studies.** The biodistribution of the four ^{18}F-labeled TOCA analogs 10 and 60 min postinjection (p.i.) was determined in AR42J tumor-bearing nude mice (Table 4).

All of the compounds showed rapid elimination from the blood pool and were mainly cleared via the kidneys. Activity levels in the kidneys 60 min p.i. were comparable for Gluc-Lys([^{18}F]FP)-TOCA and both [^{18}F]FBOA analogs (7.49–9.82% of injected dose/g; %iD/g). In contrast, Gluc-*S*-Dpr([^{18}F]FP)-TOCA showed a particularly low renal activity accumulation of 1.86 ± 0.70%iD/g.

This derivative also exhibited the lowest nonspecific uptake in liver and intestine (0.23 ± 0.04 and 1.11 ± 0.13%iD/g at 60 min p.i., respectively). Whereas hepatic and intestinal accumulation 60 min p.i. were slightly higher and nearly identical for Gluc-Lys([^{18}F]FP)-TOCA and Cel-*S*-Dpr([^{18}F]FBOA)TOCA, it was significantly increased in the case of Gluc-*S*-Dpr([^{18}F]FBOA)TOCA (3.54 *versus* 0.72–0.88 and 6.96 *versus* 1.54–1.56%iD/g, respectively).

In sst-positive tissues such as stomach, pancreas, and adrenals, a decrease in activity concentration was observed between 10 and 60 min p.i. for all of the peptides, indicating a certain contribution of circulating activity to the observed uptake in

Table 3 Internalization (in % of the reference [^{125}I]TOC) of the compounds investigated in CHO[a] cells stably expressing $hsst_2$ and the $EC_{50,R}$ [= EC_{50} (^{123}I-labeled analog)/EC_{50} ([^{125}I]TOC)] of unlabeled TOC for internalization

Values are mean ± SD, number of experiments in parentheses.

Peptide	Internalization [% of [^{125}I]TOC]	$EC_{50,R}$
[^{123}I]Gluc-*S*-Dpr(FP)TOCA	190.2 ± 6.6 (3)	3.21 ± 0.12 (3)
[^{123}I]Gluc-*S*-Dpr(FBOA)TOCA	139.3 ± 2.4 (2)	3.24 ± 0.13 (2)
[^{123}I]Cel-*S*-Dpr(FBOA)TOCA	162.6 ± 7.8 (3)	4.10 ± 0.17 (3)

[a]CHO, Chinese hamster ovary.

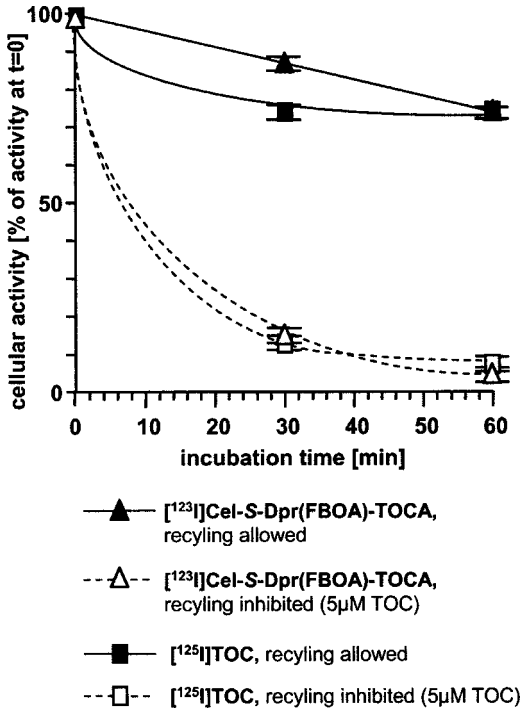

Fig. 3 Exemplary externalization of [^{123}I]Cel-*S*-Dpr(FBOA)TOCA and the reference [^{125}I]TOC from Chinese hamster ovary cells stably expressing $hsst_2$ under conditions allowing (no TOC in the external medium) and inhibiting (5 μM TOC in the external medium) ligand recycling ($n = 3$); *bars,* ±SD.

Table 4 Biodistribution of Gluc-Lys([^{18}F]FP)TOCA, Gluc-*S*-Dpr([^{18}F]FP)TOCA, Gluc-*S*-Dpr([^{18}F]FBOA)TOCA, and Cel-*S*-Dpr([^{18}F]FBOA)TOCA in AR42J rat pancreatic tumor bearing nude mice 10 and 60 min p.i. (n = 4–5)

	Gluc-Lys([^{18}F]FP)TOCA		Gluc-*S*-Dpr([^{18}F]FP)TOCA		Gluc-*S*-Dpr([^{18}F]FBOA)TOCA		Cel-*S*-Dpr([^{18}F]FBOA)TOCA	
	10 min p.i.[a]	60 min p.i.	10 min p.i.	60 min p.i.	10 min p.i.	60 min p.i.	10 min p.i.	60 min p.i.
Blood	2.58 ± 0.31	0.54 ± 0.06	3.15 ± 1.09	0.12 ± 0.03	5.58 ± 0.53	0.96 ± 0.24	4.41 ± 0.40	0.57 ± 0.09
Liver	1.89 ± 0.11	0.72 ± 0.14	1.57 ± 0.58	0.23 ± 0.04	16.96 ± 2.03	3.54 ± 0.88	4.88 ± 0.70	0.88 ± 0.12
Intestine	1.57 ± 0.26	1.88 ± 0.52	1.54 ± 0.44	1.11 ± 0.13	2.69 ± 0.49	6.96 ± 1.22	1.58 ± 0.16	1.56 ± 0.15
Kidney	17.47 ± 3.32	8.69 ± 1.09	16.57 ± 5.95	1.86 ± 0.70	30.01 ± 5.74	9.82 ± 2.97	26.70 ± 3.53	7.49 ± 0.56
Spleen	n.d.	n.d.	0.83 ± 0.27	0.11 ± 0.03	1.83 ± 0.18	0.56 ± 0.14	1.09 ± 0.16	0.24 ± 0.06
Muscle	0.68 ± 0.12	0.24 ± 0.03	0.65 ± 0.16	0.05 ± 0.03	0.84 ± 0.07	0.16 ± 0.04	0.86 ± 0.43	0.12 ± 0.03
Lung	n.d.	n.d.	2.94 ± 1.00	0.51 ± 0.08	5.93 ± 0.31	1.97 ± 0.39	4.90 ± 0.06	1.15 ± 0.23
Femur	n.d.	n.d.	1.23 ± 0.32	0.33 ± 0.07	1.44 ± 0.14	0.52 ± 0.09	1.34 ± 0.29	0.64 ± 0.04
Stomach	3.56 ± 0.27	3.07 ± 0.14	6.05 ± 0.89	4.82 ± 0.70	5.20 ± 1.08	3.97 ± 0.60	5.84 ± 0.86	6.02 ± 1.12
Pancreas	3.20 ± 0.32	2.32 ± 0.11	8.05 ± 1.43	4.78 ± 0.76	4.26 ± 0.87	3.28 ± 0.48	7.15 ± 1.12	5.19 ± 0.68
Adrenals	2.10 ± 0.32	0.86 ± 0.20	2.87 ± 0.63	1.18 ± 0.27	4.00 ± 0.70	1.20 ± 0.21	3.23 ± 0.38	1.45 ± 0.25
Tumor	11.52 ± 2.44	13.54 ± 1.47	9.63 ± 2.18	15.08 ± 1.45	15.85 ± 2.24	21.80 ± 1.35	13.54 ± 2.69	24.04 ± 2.54

[a]p.i., postinjection; n.d., not determined.

these organs. The highest ligand accumulation 60 min p.i. was found for Cel-*S*-Dpr([^{18}F]FBOA)TOCA (6.02 ± 1.12, 5.19 ± 0.68 and 1.45 ± 0.25%iD/g in stomach, pancreas, and adrenals, respectively).

In contrast to the other sst-expressing tissues, tumor accumulation of all four of the analogs increased with time. It was comparable both for the [^{18}F]FP-pair as well as for the [^{18}F]FBOA-pair at both time points. However, the tumor uptake observed for Gluc-*S*-Dpr([^{18}F]FBOA)TOCA and in particular for Cel-*S*-Dpr([^{18}F]FBOA)TOCA was significantly higher than that of the two [^{18}F]FP-analogs (21.8 and 24.0 *versus* 13.5 and 15.1%iD/g at 60 min p.i., respectively).

High tumor:nontumor ratios, which are indispensable for high-contrast PET imaging of sst-expressing malignancies, were not only observed for Cel-*S*-Dpr([^{18}F]FBOA)TOCA with its very high tumor accumulation (24.0 ± 2.5%iD/g at 60 min p.i.) but were even higher for Gluc-*S*-Dpr([^{18}F]FP)TOCA (15.1 ± 1.5%iD/g at 60 min p.i.; Fig. 4). Due to the particularly low activity levels found in blood, liver, intestine, and kidney for Gluc-*S*-Dpr([^{18}F]FP)TOCA, tumor:organ ratios 60 min p.i. were 123:1, 66:1, 14:1, and 8:1, respectively, for these organs. For Cel-*S*-Dpr([^{18}F]FBOA)TOCA, values were 42:1, 27:1, 15:1, and 3:1 for blood, liver, intestine, and kidney, respectively.

The tumor:kidney ratios determined via ROI analysis of PET images obtained ~60 min p.i. of Gluc-*S*-Dpr([^{18}F]FP)-TOCA, Gluc-*S*-Dpr([^{18}F]FBOA)TOCA, and Cel-*S*-Dpr([^{18}F]-FBOA)TOCA (Fig. 5) are in accordance with the data determined in the biodistribution studies (7.2 *versus* 8.1, 1.9 *versus* 2.2, and 1.4 *versus* 3.2, respectively).

To determine the specificity of radioligand accumulation in tumor and other sst-expressing tissues, the biodistribution of all four of the ^{18}F-labeled TOCA analogs was also determined 60 min after coinjection of 15 μg of unlabelled TOC. Under these conditions, tumor accumulation of the four derivatives investigated was reduced to 18% (Gluc-*S*-Dpr([^{18}F]FP)TOCA and Cel-*S*-Dpr([^{18}F]FBOA)TOCA), 26% (Gluc-*S*-Dpr([^{18}F]FBOA)TOCA), and 30% (Gluc-Lys([^{18}F]FP)TOCA) of control (Fig. 6), demonstrating a high extent of somatostatin receptor-mediated uptake. In

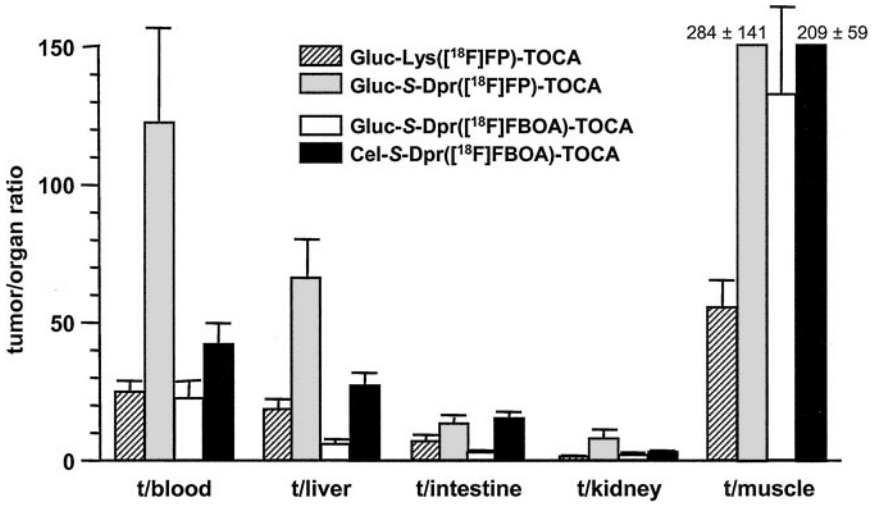

Fig. 4 Tumor:organ ratios of [Gluc-Lys([^{18}F]FP)-TOCA], Gluc-*S*-Dpr([^{18}F]FP)TOCA, Gluc-*S*-Dpr([^{18}F]FBOA)TOCA, and Cel-*S*-Dpr([^{18}F]FBOA)TOCA in AR42J tumor-bearing nude mice 60 min p.i. (n = 4–5); *bars*, ±SD.

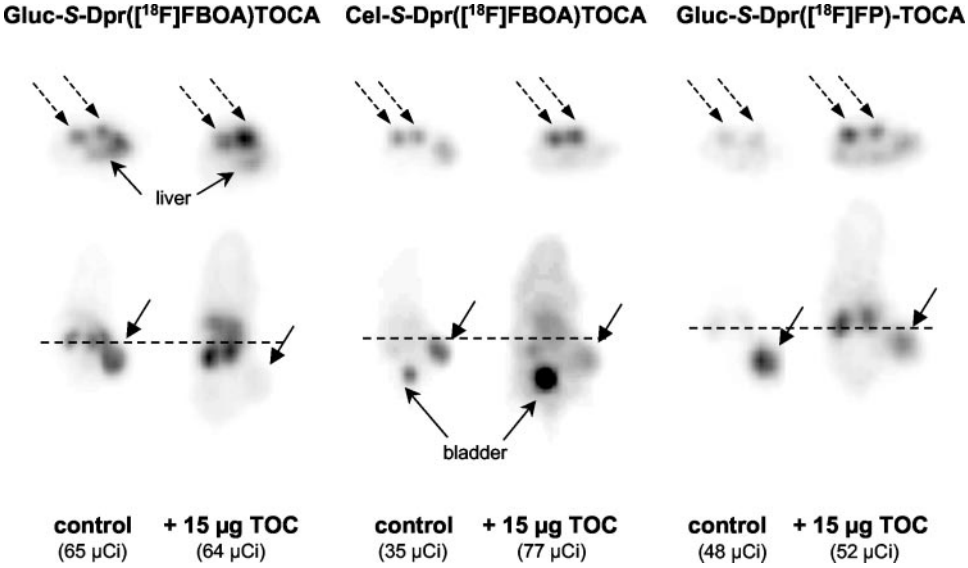

Fig. 5 Axial (*top images*) and coronar (*bottom images*) positron emission tomography images of AR42J tumor-bearing nude mice 60 min p.i. of Gluc-*S*-Dpr([^{18}F]FP)TOCA (*left*) and 45–65 min p.i. of Gluc-*S*-Dpr([^{18}F]FBOA)TOCA (*center*), and Cel-*S*-Dpr([^{18}F]-FBOA)TOCA (*right*). For control, only the ^{18}F-labeled peptides were injected. For blocking studies, 15 μg of cold Tyr^3-octreotide (TOC) were coinjected. The amount of activity injected is given in *parentheses*. *Solid arrows* indicate the tumor; *dashed arrows* indicate the kidneys. The ---- in the coronar images represents the plane of the axial image above.

pancreas and stomach, activity levels were reduced to a lower extent (38–49% and 30–61% of control, respectively), whereas in adrenals and lung, organs known to also express somatostatin receptors, ligand accumulation was even increased under blocking conditions (up to 240% of control; data not shown). The effect of coadministration of a blocking dose of TOC was also demonstrated in PET studies using a conventional PET scanner (Fig. 5).

DISCUSSION

On the basis of its pharmacokinetic profile, Gluc-Lys([^{18}F]FP)-TOCA is ideally suited for *in vivo* somatostatin receptor imaging using PET. It shows rapid renal elimination from the circulation and very high tumor accumulation even at early time points after injection (<30 min; Ref. 22). However, clinical routine applicability of PET radiopharmaceuticals does not only rely on their *in vivo* imaging properties but also on the possibility of fast and high-yield radiosynthesis, prerequisites that are not fulfilled for Gluc-Lys([^{18}F]FP)-TOCA. Radiochemical yields of the five-step synthesis are comparably low (20–30%), partly due to long reaction times (~3 h). The recent development of a high-yield two-step radiohalogenation method via chemoselective oxime formation between an aminooxy-functionalized peptide and a radiohalogenated aldehyde or ketone (28; see footnote 5) offers new perspectives for large-scale radioflourination of octreotide analogs and other bioactive peptides for clinical PET studies. Therefore, it was the aim of this study to exploit the advantages of this new ^{18}F-labeling methodology as well as the potency of glycosylation as a chemical tool to improve peptide pharmacokinetics (16–22; see footnote 4) for the development of new carbohydrated ^{18}F-labeled octreotide derivatives suitable for routine application in PET imaging of sst-overexpressing human malignancies.

The evaluation of the three new ^{18}F-labeled TOCA derivatives presented in this study, Gluc-*S*-Dpr([^{18}F]FP)TOCA, Gluc-*S*-Dpr([^{18}F]FBOA)TOCA, and Cel-*S*-Dpr([^{18}F]FBOA)-TOCA (Fig. 1), in comparison with the reference Gluc-Lys([^{18}F]FP)-TOCA, was focused on several aspects, including ease of precursor synthesis and radiolabeling, and influence of both carbohydration- and radiolabeling method on *in vitro* ligand internalization and residualization in sst-expressing cells and *in vivo* pharmacokinetics.

From a synthetic and structural point of view, glycosylation via Maillard reaction and subsequent Amadori rearrangement used in the case of Gluc-Lys([^{18}F]FP)TOCA has the inherent disadvantage of affording a variety of glycosylated conformers. In Gluc-Lys([^{18}F]FP)TOCA, the α- and β-furanoid, as well as the open-chain conformations of the deoxy-ketoses are possible beside the β-pyranoid structure depicted in Fig. 1 and may be present in equilibrium mixtures (39). It has been demonstrated,

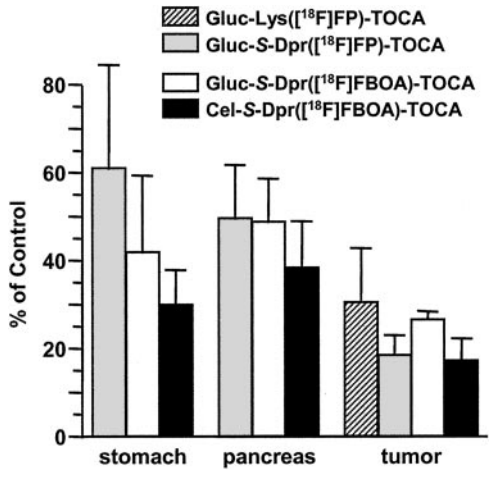

Fig. 6 Effect of coinjection of 15 μg of cold Tyr^3-octreotide the uptake of [Gluc-Lys([^{18}F]FP)-TOCA], Gluc-*S*-Dpr([^{18}F]FP)-TOCA, Gluc-*S*-Dpr([^{18}F]FBOA)TOCA, and Cel-*S*-Dpr([^{18}F]FBOA)-TOCA in tumor, pancreas, and stomach of AR42J tumor-bearing nude mice 60 min p.i. (n = 3); *bars*, ±SD.

however, that in the case of radioiodinated TOC and TOCA derivatives glycosylation via Amadori reaction not only allows "fine tuning" of the lipophilicity of the ligands and, thus, excretion characteristics. In contrast to their maltose and maltotriose counterparts, the glucose Amadori products ([^{123}I]Gluc-TOC and [^{123}I]Gluc-TOCA) exhibited significantly enhanced sst_2-mediated ligand internalization *in vitro*. *In vivo*, both [^{123}I]Gluc-TOCA and especially the maltotriose analog [^{123}I]Mtr-TOCA showed substantially increased tumor accumulation compared with [^{123}I]TOCA (22).[4,6]

For a more precise assessment of the influence of carbohydrate structure on the physicochemical and pharmacokinetic properties of radiolabeled octreotide analogs, a glycosylation method yielding glycopeptides with known sugar conformation was needed. This prerequisite was met by the use of *S*-glycosylated 3-mercaptopropionic acid as a glycosyl donor (40). Use of sugar 1,2-*trans* peracetate precursors results in the formation of the β-thioglycoside exclusively and, thus, glycopeptides with known sugar conformation. Furthermore, compared with glycosylation via Amadori reaction, peptide conjugation with *S*-glycosylated 3-mercaptopropionic acid has the distinct advantage of a much greater ease of synthesis, *i.e.*, shorter reaction times (30 min *versus* 16 h), higher glycosylation yields (>99% *versus* ~80%), and a significantly lower proportion of side product formation.

With respect to the efficiency of peptide ^{18}F-labeling, the present as well as previous studies (see footnote 5) clearly illustrate the excellence of chemoselective oxime formation over other prosthetic group radiofluorination strategies (13). The present method allows large-scale radiofluorination of peptides in high yields and offers unprecedented flexibility both with respect to the radiohalogenation precursor as well as to the nature of the radiohalogenated aldehyde or ketone used.

On a clinical basis, the applicability of ^{18}F-labeled octreotide analogs for high-contrast somatostatin receptor imaging using PET crucially relies on three factors, including fast and efficient radioligand accumulation in target tissue, sufficient ligand retention, and rapid elimination from the circulation and nontarget organs. Whereas the latter is greatly influenced by general physicochemical properties of the radioligand molecule such as lipophilicity or net charge, the first two mainly depend on the efficiency of receptor-mediated ligand internalization.

The amount of internalized receptor-agonist complex can be influenced both on the level of cellular receptor regulation and on the basis of radioligand structure. It has been shown that both *in vitro* and *in vivo* chronic agonist treatment can lead to receptor up-regulation and, thus, enhanced radioligand internalization (41–43). On the basis of radioligand structure, comparative studies including a variety of radiometallated (^{111}In and ^{64}Cu) Phe^3-octreotide, TOC, and TOCA derivatives, as well as radioiodinated sugar analogs of TOC and TOCA, revealed that ligand internalization is influenced by the nature of the chelate (DOTA) and can be substantially increased by Phe^3-for-Tyr^3 substitution and even more so by terminal Thr(ol)^8-for-Thr^8 exchange (5, 20, 21, 44).[4,6] Furthermore, certain sugar residues were also shown to enhance ligand internalization.[6] Whereas in many cases increased internalization is paralleled by an increased receptor affinity, octreotide analogs with comparable binding affinity were also found to exhibit considerable differences in internalization efficiency (44, 45).[6]

The same observations were made in the internalization studies performed with [^{123}I]Gluc-*S*-Dpr(FP)TOCA, [^{123}I]Gluc-*S*-Dpr(FBOA)TOCA, and [^{123}I]Cel-*S*-Dpr(FBOA)TOCA (Table 3). In the case of [^{123}I]Cel-*S*-Dpr(FBOA)TOCA and [^{123}I]Gluc-*S*-Dpr(FBOA)TOCA, the increased internalization (*i.e.*, the amount of internalized activity) of the cellobiose compared with the corresponding glucose analog is accompanied by a significantly higher $EC_{50,R}$. That these two quantities correlate has already been demonstrated in a previous study with a series of glycosylated, radioiodinated TOC and TOCA analogs.[6] In contrast to data obtained in the aforementioned study, however, the increased $EC_{50,R}$ of [^{123}I]Cel-*S*-Dpr(FBOA)TOCA compared with its Gluc-counterpart also correlates with higher sst_2-affinity (Table 2).

Interestingly, [^{123}I]Gluc-*S*-Dpr(FP)TOCA shows an $EC_{50,R}$ value and a sst_2 affinity nearly identical to that of [^{123}I]Gluc-*S*-Dpr(FBOA)TOCA but a 1.4-fold enhanced internalization. The only structural difference between these two peptides consists in the size (FP < FBOA) and type (aliphatic *versus* aromatic) of the prosthetic group anchored to the Dpr^0-side chain. In contrast to the significant improvement of receptor affinity by the transition from [^{123}I]Gluc- to [^{123}I]Cel-*S*-Dpr-(FBOA)TOCA, replacement of the small FP group in [^{123}I]-Gluc-*S*-Dpr(FP)TOCA by the bulky aromatic FBOA group has no detectable influence on peptide receptor affinity, but it reduces ligand internalization. Therefore, it seems probable, that beside receptor affinity, ligand geometry also plays a significant role with respect to the internalization efficiency of radiolabeled octreotide derivatives.

Overall, radioligand accumulation inside tumor cells is not only determined by the extent of ligand internalization but also by the rates of externalization and subsequent reinternalization (recycling) and/or intracellular degradation of the radioligand. In externalization studies performed both under conditions allowing and inhibiting recycling (Fig. 3), the washout of [^{123}I]Gluc-*S*-Dpr(FP-)TOCA, [^{123}I]Gluc-*S*-Dpr(FBOA)TOCA, and [^{123}I]Cel-*S*-Dpr(F-BOA)TOCA from tumor cells was found to be nearly identical and comparable with that of [^{125}I]TOC. Thus, neither glycosylation nor the radiolabeling method have a detectable influence on externalization kinetics. These findings are in accordance with data from Koenig *et al.* (46), which demonstrated agonist-independent rates of externalization for intact radiolabeled somatostatin analogs. The fact that for all of the fluorinated TOCA derivatives >96% of the initial cellular activity was externalized within 60 min under conditions inhibiting recycling (5 μM TOC) indicates a negligible extent of intracellular ligand residualization. This represents one major disadvantage of radiohalogenated over radiometallated octreotide analogs, of which the charged radiometal-chelate-containing fragments remain trapped in the lysosomal compartments after degradation (7, 47, 48). The high extent of apparent intracellular retention of [^{123}I]Gluc-*S*-Dpr(FP)TOCA and the two FBOA-analogs under conditions allowing recycling, however, demonstrate efficient reinternalization of externalized activity. This fact may contribute to the observed increase in *in vivo* tumor accumulation of all of the ^{18}F-labeled TOCA derivatives in this study between 10 and 60 min p.i. despite the drastic reduction of blood activity levels and, thus, ligand availability during this time period. To improve "real" intracellular retention of radiohalogenated peptides, how-

ever, the use of negatively charged prosthetic groups seems a promising approach (49).

In contrast to data from other studies (21),[6] this study demonstrates that *in vitro* internalization as well as $EC_{50,R}$ values only have limited predictive power with respect to *in vivo* tumor accumulation of the radioligands investigated. On the basis of the *in vitro* data, and assuming comparable biokinetics of the ^{18}F-labeled peptides, similar and high tumor accumulation would have been expected for Gluc-*S*-Dpr([^{18}F]FP)TOCA and Cel-*S*-Dpr([^{18}F]FBOA)TOCA, and a slightly lower accumulation of Gluc-*S*-Dpr([^{18}F]FBOA)TOCA. Unexpectedly, tumor uptake of the two [^{18}F]FBOA derivatives was very high and comparable at all of the time points investigated, whereas it was 35% lower in the case of Gluc-*S*-Dpr([^{18}F]FP)TOCA (Table 4). One possible explanation for this divergence, beside a major contribution of general ligand pharmacokinetics on *in vivo* tumor accumulation, may be the use of cells expressing the human sst_2-receptor bearing an N-terminal hemagglutinin epitope tag for the *in vitro* experiments, whereas the biodistribution studies were performed using the rat pancreatic acinar tumor model AR42J. For [^{123}I]Gluc-TOCA, fundamentally different internalization characteristics and $EC_{50,R}$ values were found when CHO ($hsst_2$) and AR42J cells were used for the *in vitro* experiment, respectively.[6] Because no significant effect of radioiodination of Tyr^3 in TOC on sst_2-affinity was observed (Table 2), it is unlikely that the use of the radioiodinated ^{19}F-reference compounds instead of the ^{18}F-labeled peptides in the internalization studies may have had an influence on the internalization characteristics of the respective radioligands *in vitro*.

That the accumulation of the four ^{18}F-labeled TOCA analogs in tumor and other somatostatin receptor-positive tissues is predominantly receptor mediated was confirmed by *in vivo* competition studies (Figs. 5 and 6). Coinjection of an excess of unlabelled TOC led to a reduction of tumor uptake to 26–30% [Gluc-Lys([^{18}F]FP)TOCA and Gluc-*S*-Dpr([^{18}F]FBOA)-TOCA] and 18% [Gluc-*S*-Dpr([^{18}F]FP)TOCA and Cel-*S*-Dpr([^{18}F]FBOA)TOCA] of controls. In stomach and pancreas, ligand uptake was reduced to 30–60% and 38–48% of controls, respectively, for the peptides investigated. Generally, a comparably low dose of cold competitor was administered in this study (10–15 μg TOC per mouse) due to severe toxic side effects (cyanosis and swelling of paws and eyes in 50% of the cases followed by death in <30 min p.i.) observed in the Swiss *nu/nu* mice used, when higher doses were applied. This might explain the seemingly high extent of nonblockable accumulation of the ^{18}F-labeled peptides in sst-expressing tissues. In other studies applying 50–100 μg of peptide per mouse, tumor uptake was reduced to a minimum of 7% (50) and 15% (21) of control. Interestingly, no significant extent of receptor-mediated ligand uptake was detected for any of the ^{18}F-labeled TOCA derivatives in lung and adrenals, organs that have been shown to express somatostatin receptors (51, 52). These findings are in contradiction to results obtained with radioiodinated glucosylated TOC and TOCA analogs, as well as ^{64}Cu-labeled triethylenetetramine-TOCA. In both studies, lung accumulation in nude mice was effectively blocked by coadministration of unlabeled competitor (21, 53).

Altogether, the applicability of an ^{18}F-labeled octreotide analog for rapid and high-contrast PET imaging is not only determined by its absolute accumulation in target tissues, but also by the rate of elimination from the circulation and excretion organs and, thus, the achievable target:nontarget tissue ratios. It has been demonstrated for a series of glycosylated, radioiodinated TOC derivatives that the extent of hepatic and intestinal accumulation correlates with ligand lipophilicity (19). The same applies to the corresponding radioiodinated glucose-, maltose- and maltotriose-TOCA-analogs,[4] [^{125}I]TOCA, [^{125}I]Gluc-TOCA, [^{125}I]Malt-TOCA, and [^{125}I]Mtr-TOCA, and also to the four ^{18}F-labeled TOCA derivatives investigated in this study (Fig. 7). Interestingly, this correlation seems to be almost inde-

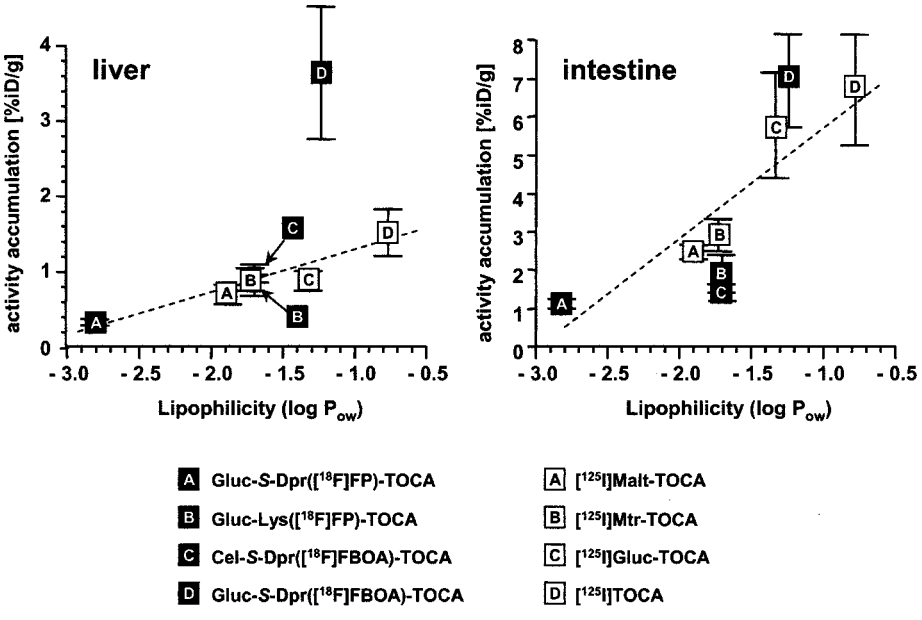

Fig. 7 Correlation between the lipophilicity (log P_{ow}; $n = 6$) of glycosylated, radiohalogenated Tyr^3-octreotate (*TOCA*) analogs and their activity accumulation in liver (*left*) and intestine (*right*) of AR42J tumor-bearing nude mice 60 min p.i. (n = 3–5); *bars*, ±SD

pendent of the radiohalogenation or glycosylation method. Gluc-Lys([^{18}F]FP)TOCA and Cel-*S*-Dpr([^{18}F]FBOA)TOCA differ in both respects and, thus, in ligand geometry and net charge. Nevertheless, they have identical lipophilicities and, thus, show an identical biodistribution in the excretion organs 60 min p.i. (Table 4). Only in Gluc-*S*-Dpr([^{18}F]FBOA)TOCA, the aromatic [^{18}F]FBOA group seems to structurally outweigh the sugar residue and, thus, leads to overproportional accumulation of this ligand in liver, intestine, and kidney.

It is generally assumed that charge-dependent endocytosis significantly contributes to the renal uptake of small bioactive peptides (54). The fact that kidney accumulation of radiometallated octreotide derivatives can be efficiently reduced by coinfusion of cationic amino acids during internal radiotherapy additionally supports this assumption (3, 55). A lower positive net charge of the peptide should, therefore, result in reduced kidney accumulation (56). This seems to be the case for Gluc-*S*-Dpr([^{18}F]FP)TOCA in comparison with Gluc-Lys([^{18}F]FP)TOCA: the loss of the positive charge on N_α of the N-terminal amino acid leads to a reduction in kidney accumulation to ~20% of the value found for the Amadori compound. On the other hand, net charge is also reduced in the case of the two [^{18}F]FBOA analogs, but renal activity levels remain almost unchanged compared with Gluc-Lys([^{18}F]FP)TOCA. This observation suggests a significant additional "inverse" contribution of ligand geometry, in this case the presence of the bulky aromatic FBOA-moiety, on kidney accumulation.

In conclusion, two of the ^{18}F-labeled octreotates investigated in this study, Gluc-*S*-Dpr([^{18}F]FP)TOCA and Cel-*S*-Dpr([^{18}F]FBOA)TOCA, show excellent pharmacokinetic profiles optimal for *in vivo* PET imaging of sst-positive tumors. Their particularly high tumor:background ratios render them vastly superior to the most promising ^{18}F-labeled octreotide analog developed thus far, Gluc-Lys([^{18}F]FP)TOCA, of which the potency in high-contrast PET imaging has already been demonstrated in first patient studies. However, the inefficiency and impracticability of [^{18}F]fluoroacylation with respect to routine ^{18}F-peptide labeling prevent application of Gluc-*S*-Dpr([^{18}F]FP)TOCA in a clinical setting. In contrast, the development of the fast, chemoselective, and high-yield two-step methodology of peptide radiofluorination via oxime formation allows rapid preparation of high amounts of Cel-*S*-Dpr([^{18}F]FBOA)TOCA, making this peptide, along with its excellent pharmacokinetics, a most promising tracer for routine PET somatostatin receptor imaging.

We assume that both the above radiohalogenation strategy based on chemoselective oxime formation as well as its combination with glycosylation using a trifunctional linker concept will provide access to a large variety of ^{18}F-, $^{123/125/131}$I-, or ^{211}At-labeled bioactive peptides with optimized pharmacokinetics for *in vivo* receptor imaging as well as peptide receptor radiotherapy.

ACKNOWLEDGMENTS

We thank Claudia Bodenstein, Brigitte Dzewas, and Coletta Kruschke for excellent technical assistance. Furthermore, we thank Wolfgang Linke for supplying 2-[^{19}F]fluoropropionic acid for the synthesis of the reference peptides.

REFERENCES

1. Wester HJ, Brockmann J, Rösch F, et al. PET-pharmacokinetics of ^{18}F-Octreotide: A comparison with ^{67}Ga-DFO-octreotide and ^{86}Y-DTPA-octreotide. Nucl Med Biol 1997;24:275–86.

2. Rösch F, Herzog H, Stolz B, et al. Uptake kinetics of the somatostatin receptor ligand [^{86}Y]DOTA-DPhe^1-Tyr^3-octreotide ([^{86}Y]SMT487) using positron emission tomography in non-human primates and calculation of radiation doses of the 90Y-labelled analogue. Eur J Nucl Med 1999;26:358–66.

3. Jamar F, Barone R, Mathieu I, et al. ^{86}Y-DOTA^0-d-Phe^1-Tyr^3-octreotide (SMT487) –a phase 1 clinical study: pharmacokinetics, biodistribution and renal protective effect of different regimens of amino acid coinfusion. Eur J Nucl Med Mol Imaging 2003;30:510–8.

4. Lewis JS, Lewis MR, Cutler PD, et al. Radiotherapy and dosimetry of ^{64}Cu-TETA-Tyr^3-octreotate in a somatostatin receptor-positive, tumor-bearing rat model. Clin Cancer Res 1999;5:3608–16.

5. Lewis JS, Lewis MR, Srinivasan A, Schmidt MA, Wang J, Anderson CJ. Comparison of four ^{64}Cu-labeled somatostatin analogues in vitro and in a tumor-bearing rat model: evaluation of new derivatives for positron emission tomography imaging and targeted radiotherapy. J Med Chem 1999;42:1341–7.

6. Anderson CJ, Dehdashti F, Cutler PD, et al. ^{64}Cu-TETA-octreotide as a PET imaging agent for patients with neuroendocrine tumors. J Nucl Med 2001;42:213–21.

7. Froidevaux S, Eberle AN, Christe M, et al. Neuroendocrine tumor targeting: study of novel gallium-labeled somatostatin radiopeptides in a rat pancreatic tumor model. Int J Cancer 2002;98:930–7.

8. Hofmann M, Maecke H, Borner R, et al. Biokinetics and imaging with the somatostatin receptor PET radioligand (68)Ga-DOTATOC: preliminary data. Eur J Nucl Med 2001;28:1751–7.

9. Henze M, Schuhmacher J, Hipp P, et al. PET imaging of somatostatin receptors using [^{68}Ga]DOTA-d-Phe^1-Tyr^3-octreotide: First results in patients with meningiomas. J Nucl Med 2001;42:1053–6.

10. Ugur O, Kothari PJ, Finn RD, et al. Ga-66 labeled somatostatin analogue DOTA-dPhe^1-Tyr^3-octreotide as a potential agent for positron emission tomography imaging and receptor mediated internal radiotherapy of somatostatin receptor positive tumors. Nucl Med Biol 2002;29:147–57.

11. Eisenwiener KP, Prata MI, Buschmann I, et al. NODAGATOC, a new chelator-coupled somatostatin analogue labeled with [$^{67/68}$Ga] and [^{111}In] for SPECT, PET, and targeted therapeutic applications of somatostatin receptor (hsst2) expressing tumors. Bioconjug Chem 2002;13:530–41.

12. Lundqvist H, Tolmachev V. Targeting peptides and positron emission tomography. Biopolymers (Pept Sci) 2002;66:381–92.

13. Okarvi SM. Recent progress in fluorine-18 labelled peptide radiopharmaceuticals. Eur J Nucl Med 2001;28:929–38.

14. Guhlke S, Wester HJ, Bruns C, Stöcklin G. (2-[^{18}F]fluoropropionyl-(D)phe^1)-octreotide, a potential radiopharmaceutical for quantitative somatostatin receptor imaging with PET: synthesis, radiolabeling, in vitro validation and biodistribution in mice. Nucl Med Biol 1994;21:819–25.

15. Hostetler ED, Edwards WB, Anderson CJ and Welch MJ. J Labelled Compd. Radiopharm 1999;42 (Suppl 1): 720–2.

16. Leisner M, Kessler H, Schwaiger M, Wester H-J Synthesis of Nα-d-Phe^1-amadori derivatives of Tyr^3-octreotide: Precursors for ^{123}I-/^{18}F-labeled sstr-binding SPECT/PET tracers with improved biodistribution. J Labeled Compd Radiopharm 1999;42:549–51.

17. Haubner R, Wester HJ, Weber WA, et al. Noninvasive imaging of alpha(v)beta3 integrin expression using ^{18}F-labeled RGD-containing glycopeptide and positron emission tomography. Cancer Res 2001;61:1781–5.

18. Haubner R, Wester HJ, Burkhart F, et al. Glycosylated RGD-containing peptides: tracer for tumor targeting and angiogenesis imaging with improved biokinetics. J Nucl Med 2001;42:326–36.

19. Schottelius M, Wester HJ, Reubi JC, Senekowitsch-Schmidtke R, Schwaiger M. Improvement of pharmacokinetics of radioiodinated Tyr^3-octreotide by conjugation with carbohydrates. Bioconjug Chem 2002;13:1021–30.

20. Wester HJ, Schottelius M, Scheidhauer K, Reubi JC, Wolf I, Schwaiger M. Comparison of radioiodinated TOC, TOCA and Mtr-TOCA: the effect of carbohydra-tion on the pharmacokinetics. Eur J Nucl Med Mol Imaging 2002;29:28–38.

21. Vaidyanathan G, Friedman HS, Affleck DJ, Schottelius M, Wester HJ, Zalutsky MR. Specific and high-level targeting of radiolabeled octreotide analogues to human medulloblastoma xenografts. Clin Cancer Res 2003;9:1868–76.

22. Wester HJ, Schottelius M, Scheidhauer K, et al. PET imaging of somatostatin receptors: design, synthesis and preclinical evaluation of a novel ^{18}F-labelled, carbohydrated analogue of octreotide. Eur J Nucl Med 2003;30:117–22.

23. Wester HJ, Hamacher K, Stöcklin G. A comparative study of N. C. A. fluorine-18-labeling of proteins via acylation and photochemical conjugation Nucl Med Biol 1996;23:365–72.

24. Vaidyanathan G, Zalutsky MR. Labeling proteins with fluorine-18 using N-succinimidyl 4-[^{18}F]fluorobenzoate. Int J Rad Appl Instrum 1992;(B 19):275–81.

25. Fredriksson A, Ekberg K, Ingvar M, Johansson BL, Wahren J, Stone-Elander S. In vivo biodistribution and pharmacokinetics of (18)F-labeled human C-peptide: evaluation in monkeys using positron emission tomography. Life Sci 2002;71:1361–70.

26. Bergmann R, Scheunemann M, Heichert C, et al. Biodistribution and catabolism of (18)F-labeled neurotensin(8–13) analogs. Nucl Med Biol 2002;29:61–72.

27. Kurth M, Pelegrin A, Rose K, et al. Site-specific conjugation of a radioiodinated phenethylamine derivative to a monoclonal antibody results in increased radioactivity localization in tumor. J Med Chem 1993;36:1255–61.

28. Thumshirn G, Hersel U, Goodman SL, Kessler H. Multimeric cyclic RGD peptides as potential tools for tumor targeting: solid-phase peptide synthesis and chemoselective oxime ligation. Chemistry Eur J 2003;9:2717–2725.

29. Elofsson M, Walse B, Kihlberg J. Building blocks for glycopeptide synthesis: Glycosylation of 3-mercapropropionic acid and fmoc amino acids with unprotected carboxyl groups. Tetrahedron Lett 1991;32:7613–6.

30. Shin I, Park K. Solution phase synthesis of aminooxy peptoids in the *C* to *N* and *N* to *C* directions. Org Lett 2002;4:869–72.

31. Herzig J, Nudelman A, Gottlieb HE, Fisher B. Studies in sugar chemistry. 2. A simple method for O-deacylation of polyacylated sugars. J Org Chem 1986;51:727–30.

32. Albert R, Marbach P, Bauer W, et al. SDZ CO 611: A highly potent glycosylated analog of somatostatin with improved oral acitivity Life Sci 1993;53:517–25.

33. Bergmann ED, Blank I. Studies on organic fluorine compounds part I: Some esters of monofluoroacetic acid and related compounds. J Am Chem Soc 1953;75:3786.

34. Iwata R, Pascali C, Bogni A, et al. A new, convenient method for the preparation of 4-[^{18}F]fluorobenzyl halides. Appl Radiat Isotopes 2000;52:87–92.

35. Buchwald P, Bodor N. Octanol-water partition of nonzwitterionic peptides: predictive power of a molecular size-based model. Proteins: Structure, Function and Genetics 1998;30:86–99.

36. Reubi JC, Schär JC, Waser B, et al. Affinity profiles for human somatostatin receptor subtypes SST1-SST5 of somatostatin radiotracers selected for scintigraphic and radiotherapeutic use Eur. J Nucl Med 2000;27:273–82.

37. Viguerie N, Tahari-Jouti N, Esteve JP, et al. Functional somatostatin receptors on a rat pancreatic acinar cell line. Am J Physiol 1988; 255:G113–20.

38. Buré, C. Lelièvre D, Delmas A. Identification of by-products from an orthogonal peptide ligation by oxime bonds using mass spectrometry and tandem mass spectrometry. Rapid Commun Mass Spectrom 2000; 14:2158–64.

39. Funcke W. ^{13}C-NMR-Untersuchungen an Mutarotationsgemischen C-6- und C-4- sowie C-6-modifizierter Amadoriverbindungen Liebigs Ann Chem 1978;2099–104.

40. Elofsson M, Roy S, Walse B, Kihlberg J. Solid-phase synthesis and conformational studies of glycosylated derivatives of helper-T-cell immunogenic peptides from hen-egg lysozyme. Carbohydrate Res 1993; 246:89–103.

41. Hukovic N, Panetta R, Kumar U, Patel YC. Agonist-dependent regulation of cloned human somatostatin receptor types 1–5 (hSSTR1–5): Subtype selective internalization or upregulation. Endocrinology 1996;137:4046–9.

42. Froidevaux S, Hintermann E, Török M, Mäcke HR, Beglinger C, Eberle AN. Differential regulation of somatostatin receptor type 2 (sst 2) expression in AR4–2J tumor cells implanted into mice during octreotide treatment. Cancer Res 1999;59:3652–7.

43. Hofland LJ, van Koetsveld PM, Waaijers M, Zuyderwijk J, Breeman WA, Lamberts SW. Internalization of the radioiodinated somatostatin analog [^{125}I-Tyr^3]octreotide by mouse and human pituitary tumor cells: Increase by unlabeled octreotide. Endocrinology 1995;136:3698–706.

44. de Jong M, Breeman WA, Bakker WH, et al. Comparison of ^{111}In-labeled somatostatin analogues for tumor scintigraphy and radionuclide therapy. Cancer Res 1998;58:437–41.

45. Hofland LJ, Breeman WA, Krenning EP, et al. Internalization of [DOTA^0, ^{125}I-Tyr^3]octreotide by somatostatin receptor-positive cells *in vitro* and *in vivo*: implications for somatostatin receptor-targeted radioguided surgery. Proc Assoc Am Physicians 1999;111:63–9.

46. Koenig JA, Kaur R, Dodgeon I, Edwardson JM, Humphrey PP. Fates of endocytosed somatostatin sst_2 receptors and associated agonists. Biochem J 1998;336:291–8.

47. Duncan JR, Stephenson MT, Wu HP, Anderson CJ. Indium-111-diethylene-triaminepentaacetic acid-octreotide is delivered in vivo to pancreatic, tumor cell, renal, and hepatocyte lysosomes. Cancer Res 1997;57:659–71.

48. Akizawa H, Arano Y, Uezono T, et al. Renal metabolism of ^{111}In-DTPA-d-Phe^1-Octreotide in vivo. Bioconjugate Chem 1998;9:662–70.

49. Shankar S, Vaidyanathan G, Affleck D, Welsh PC, Zalutsky M. *N*-Succin-imidyl 3-[^{131}I]Iodo-4-phosphonomethylbenzoate ([^{131}I]SIPMB), a negatively charged substituent-bearing acylation agent for the radioiodination of peptides and mAbs. Bioconjugate Chem 2003;14:331–41.

50. Froidevaux S, Heppeler A, Eberle AN, et al. Preclinical comparison in AR4–2J tumor-bearing mice of four radiolabeled 1,4,7,10-tetraazacyclododecane-1,4,7,10-tetraacetic acid-somatostatin analogs for tumor diagnosis and internal radiotherapy. Endocrinology 2000;141:3304–12.

51. Bokum AMC, Rosmalen JGM, Hofland LJ, Krenning EP, van Hagen PM, Breeman WAP. Tissue distribution of octreotide binding receptors in normal mice and strains prone to autoimmunity. Nucl Med Commun 2002;23:1009–17.

52. Kraus J, Wöltje M, Schönwetter N, Höllt V. Alternative promotor usage and tissue specific expression of the mouse somatostatin receptor 2 gene. FEBS Lett 1998;428:165–70.

53. Lewis JS, Srinivasan A, Schmidt MA, Anderson CJ. In vitro and *in vivo* evaluation of ^{64}Cu-TETA-Tyr^3-octreotate A new somatostatin analog with improved target tissue uptake Nucl Med Biol 1999;26:267–73.

54. Behr TM, Goldenberg DM, Becker WS. Reducing the renal uptake of radiolabelled antibody fragments and peptides for diagnosis and therapy: present status and future limitations. Eur J Nucl Med 1998;25:201–12.

55. de Jong M, Rolleman EJ, Bernard BF, et al. Inhibition of renal uptake of indium-111-DTPA-octreotide in vivo. J Nucl Med 1996;37:1388–92.

56. Akizawa H, Arano Y, Mifune M, et al. Effect of molecular charges on renal uptake of ^{111}In-DTPA-conjugated peptides. Nucl Med Biol 2001;28:761–8.